Conference on Modelling Fluid Flow (CMFF'15)
The 16th International Conference on Fluid Flow Technologies
Budapest, Hungary, September 1-4, 2015

SIMULATION OF MULTIPLE BLUNT-BODY FLOWS WITH A HYBRID VARIATIONAL MULTISCALE MODEL

Emmanuelle Itam[1], Stephen Wornom[2], Bruno Koobus[3], Bruno Sainte-Rose[4], Alain Dervieux[5]

[1] Corresponding Author. Institut Montpelliérain Alexander Grothendieck (IMAG), Université de Montpellier, Montpellier, France, emmanuelle.itam@umontpellier.fr
[2] Société technologique LEMMA, 2000 route des Lucioles, Sophia-Antipolis, France, stephen.wornom@inria.fr
[3] IMAG, Université de Montpellier, Montpellier, France, koobus@math.univ-montp2.fr
[4] LEMMA, 11 rue de Carnot F-94270 Le Kremlin-Bicêtre, bruno.sainte-rose@lemma-ing.com
[5] Institut National de Recherche en Informatique et en Automatique (INRIA), 2004 Route des lucioles, F-06902 Sophia-Antipolis, Tel.: +33 4 92 38 77 91, E-mail: Alain.Dervieux@inria.fr

The present investigation is motivated by the simulation of high-Reynolds number massively separated flows, a challenging problem of prime interest in industry. The turbulence model is based on a hybridization strategy which blends a variational multiscale large-eddy simulation (VMS-LES) equipped with dynamic subgrid scale (SGS) models and a two-equation RANS model. The dynamic procedure (Germano) allows the adaptation of the constant of the SGS model to the spatial and temporal variation of the flow characteristics, while the VMS formulation restricts the SGS model effects to the smallest resolved scales. The hybridization strategy uses a blending parameter, such that a VMS-LES simulation is applied in region where the grid resolution is fine enough to resolve a significant part of the turbulence fluctuations, while a RANS model is acting in the regions of coarse grid resolution. The capability of the proposed hybrid model to accurately predict the aerodynamic forces acting on a circular cylinder in the supercritical regime and on tandem cylinders are investigated.

Keywords: LES, hybrid, dynamic, VMS, blunt body, cylinder, tandem

1. NOMENCLATURE

τ^{LES}	SGS stress tensor
τ^{RANS}	Reynolds stress tensor
μ_{SGS}	SGS viscosity
μ_{RANS}	RANS viscosity
l_{RANS}	RANS characteristic length
Δ	local mesh size
$\bar{C}_d$	Drag
C'_l	Lift rms fluctuations
C_p	Mean pressure coefficient
$\bar{C}_{p_b}$	Mean base pressure coefficient
St	Strouhal number
l_r	Recirculation length
D	Cylinder diameter

2. INTRODUCTION AND MOTIVATIONS

This work takes place in a study of a numerical simulation method suited to industrial problems, equipped with turbulence models adapted to the simulation of turbulent flows with massive separations and vortex shedding. Recent publications concerning this study can be found in [1],[2]. The numerical methods are of low order, applicable on unstructured tetrahedral meshes, and involve numerical dissipation. But this dissipation is made of sixth-order derivatives and very low, and advective accuracy can be as high as fifth order on Cartesian region of the mesh. The main issue which then arises is the choice of turbulence modelling which can combine well with this numerical technology.

In order to address high Reynolds number flows, we have to consider RANS-LES hybridization as in Detached Eddy Simulation (DES) [3, 4]. However DES is not designed for computing subcritical flows for which pure LES is a natural approach. Now, it is important to have a LES mode as accurate as possible. For example, the shear layer between main flow and wake can suffer from the tendancy of a Smagorinsky-like model to reinforce the filtering in these regions. Two techniques are considered to improve the accuracy of the LES component. First, the time-space strength of the filter is controlled by a dynamic process. Second, the width of the filter is numerically controlled by using a variational multiscale formulation.

The present work focuses on the following items:

- The evaluation of dynamic and hybrid VMS-LES models on the prediction of vortex shedding flows
- The simulation of the flow around circular and square cylinders : these flows involve many features and difficulties encountered in industrial problems and are studied in well documented benchmarks. They are also the first step before the computation of array of cylinders (offshore oil and gas industries, civil engineering, aeronautics)

3. NUMERICAL MODEL

The spatial discretization is based on a mixed finite-volume finite-element formulation, with degrees of freedom located at nodes i of the tetrahedrization. The finite volume part is integrated on a dual mesh built in 2D from median (Figure 1), in 3D from median plans. The diffusive fluxes are evaluated by a finite-element method, whereas a finite-volume method is used for the convective fluxes. The numerical approximation of the convective fluxes at the interface of neighboring cells is based on the Roe scheme [5].

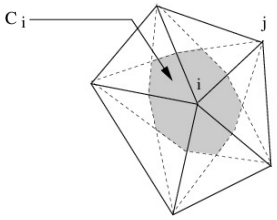

Figure 1. Dual cell in 2D

In order to obtain second-order accuracy in space, the Monotone Upwind Scheme for Conservation Laws reconstruction method (MUSCL) [6] is used, in which the Roe flux is expressed as a function of reconstructed values of the discrete flow variable W_h at each side of the interface between two cells. We refer to [7] for details on the definition of these reconstructed values. We just emphasize that particular attention has been paid to the dissipative properties of the resulting scheme since this is a key point for its successful use in LES. The numerical (spatial) dissipation provided by this scheme is made of sixth-order space derivatives [7] and this is concentrated on a narrow-band of the highest resolved frequencies. This is expected to limit undesirable damping by numerical dissipation of the large scales. Moreover, a parameter γ_S directly controls the amount of introduced viscosity and can be explicitly tuned in order to reduce it to the minimal amount needed to stabilize the simulation.

Time integration uses an implicit second-order backward differencing scheme. In [7], it is shown that when used in combination with moderate time steps, the time dissipation is also quite small.

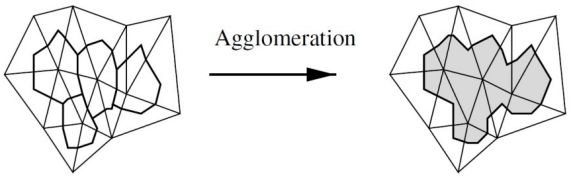

Figure 2. Building the VMS coarse level

4. TURBULENCE MODEL: VMS-LES

The Variational Multiscale (VMS) model for the large eddy simulation (LES) of turbulent flows has been introduced in [8] in combination with spectral methods. In [9], an extension to unstructured finite volumes is defined. That method is adapted in the present work. Let us explain this VMS-LES approach in a *simplified context*. Assume the mesh is made of two embedded meshes, corresponding to a P^1-continuous finite-element approximation space V_h with the usual basis functions Φ_i vanishing on all vertices but vertex i. Let be V_{2h} its embedded coarse subspace V_{2h}. Let V'_h be the complementary space: $V_h = V_{2h} \oplus V'_h$. The space of *small scales* V'_h is spanned by only the fine basis functions Φ'_i related to vertices which are not vertices of V_{2h}. We write the compressible Navier-Stokes equations as follows: $\frac{\partial W}{\partial t} + \nabla \cdot F(W) = 0$ where $W = (\rho, \rho\mathbf{u}, \rho E)$ The VMS-LES discretization writes for $W_h = \sum W_i \Phi_i$:

$$\left(\frac{\partial W_h}{\partial t}, \Phi_i\right) + (\nabla \cdot F(W_h), \Phi_i) = -\left(\tau^{LES}(W_h{}'), \Phi_i{}'\right). \quad (1)$$

For a test function related to a vertex of V_{2h}, the RHS vanishes, which limits the action of the LES term to small scales. *In practice*, embedding two unstructured meshes V_h and V_{2h} is a constraint that we want to avoid. The coarse level is then built from the agglomeration of vertices/cells as sketched in Figure 2: It remains to define the model term $\tau^{LES}(W'_h)$. This term represents the SGS stress term, acting only on small scales W'_h, and computed from the small scale component of the flow field by applying either a Smagorinsky or a WALE SGS model, [10], the constants of these models being eventually evaluated by the Germano-Lilly dynamic procedure [11, 12]. The main property of the VMS formulation is that the modeling of the unresolved structures is influencing only the small resolved scales, as described in Figure 3, in contrast with, for example the usual Smagorinsky model. This implies two main properties. First, the backscatter transfer of energy to large scales is not damped by the model. Second, the model is naturally unable to produce an artificial viscous layer at a no-slip boundary, or in shear layers.

5. TURBULENCE MODEL: HYBRID RANS/VMS-LES

The computation of massively separated flows at high Reynolds numbers on unstructured meshes

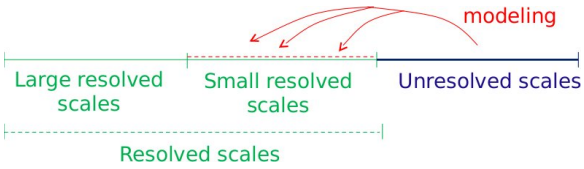

Figure 3. VMS principle

can be addressed with three families of models. Reynolds-Averaged-Navier-Stokes (RANS) is robust but shows accuracy problems in flow regions with massive separation (such as the flow around bluff-bodies). LES, and in particular our VMS-LES is more expensive than RANS, since a very fine resolution -somewhat comparable to DNS- is required in boundary layers at high Reynolds numbers. Hybrid formulations combine RANS and LES in order to exploit the advantages of the two approaches. Our goal is to build and evaluate a hybrid RANS/VMS-LES. The central idea of the proposed hybrid VMS model is to correct the mean flow field obtained with a RANS model by adding fluctuations given by a VMS-LES approach wherever the grid resolution is adequate. Our hybrid model can be shortly derived as follows.

First, let us write the semi-discretization of the RANS equations :

$$\left(\frac{\partial \langle W_h \rangle}{\partial t}, \Phi_i\right) + (\nabla \cdot F(\langle W_h \rangle), \Phi_i) = -\left(\tau^{RANS}(\langle W_h \rangle), \Phi_i\right) \quad (2)$$

in which $\langle W_h \rangle$ denotes the RANS variables.

An equation for the resolved fluctuations $W_h^c = W_h - \langle W_h \rangle$, where W_h denotes the VMS-LES variables that satisfy Eqs. (1), can then be derived by substracting Eqs. (1) and (2) :

$$\left(\frac{\partial {W_h}^c}{\partial t}, \Phi_i\right) + (\nabla \cdot F(W_h), \Phi_i) - (\nabla \cdot F(\langle W_h \rangle), \Phi_i)$$

$$= \left(\tau^{RANS}(\langle W \rangle), \Phi_i\right) - \left(\tau^{LES}({W_h}'), \Phi_i'\right) \quad (3)$$

To identify the regions where the additional fluctuations need to be computed, i.e. the regions where the grid resolution is adequate for VMS-LES, a blending function θ is introduced, which smoothly varies between 0 and 1, and which allows to recover the RANS approach for $\theta = 1$ and the VMS-LES model for $\theta = 0$. Thus Eqs. (3) become

$$\left(\frac{\partial {W_h}^c}{\partial t}, \Phi_i\right) + (\nabla \cdot F(W_h), \Phi_i) - (\nabla \cdot F(\langle W_h \rangle), \Phi_i)$$

$$= (1-\theta)\left[\left(\tau^{RANS}(\langle W \rangle), \Phi_i\right) - \left(\tau^{LES}({W_h}'), \Phi_i'\right)\right] \quad (4)$$

In order to avoid the solution of two systems of equations, Eqs (2) and (4) are recasted together as follows :

$$\left(\frac{\partial W_h}{\partial t}, \Phi_i\right) + (\nabla \cdot F(W_h), \Phi_i) = -\theta\left(\tau^{RANS}(\langle W \rangle), \Phi_i\right) - (1-\theta)\left(\tau^{LES}(W_h'), \Phi_i'\right) \quad (5)$$

where W_h denotes now the hybrid variables. The blending function $\theta = \tanh(\xi^2)$ is defined either by a prescription of the user (zonal option) or from $\xi = \mu_{SGS}/\mu_{RANS}$ or $\xi = \Delta/l_{RANS}$. The RANS component used in the proposed hybrid approach is the $k-\varepsilon$ model proposed by Goldberg and Ota [13]. The hybrid variables then write $W_h = (\rho_h, \rho_h \mathbf{u_h}, \rho_h E_h, \rho_h k_h, \rho_h \varepsilon_h)$.

6. RESULTS

For the simulations presented in this section, characteristic based conditions are used at the inflow and outflow as well as the lateral surface. In the spanwise direction, periodic boundary conditions are applied. No-slip conditions are imposed on the walls for moderate Reynolds numbers and a wall law approach is used for higher Reynolds numbers. The freestream Mach number is set to 0.1 in order to make a sensible comparison with incompressible simulations in the literature. Preconditioning is used to deal with the low-Mach number regime. For all simulations, starting from a uniform flow and once the flow is established, statistics are computed by averaging in time for, at least, 30 vortex-shedding cycles.

6.1. CIRCULAR CYLINDER - SUBCRITICAL

The presented results are compared with other LES computations [14, 15, 16] and with measurements [16, 17, 18]. The flow around a cylinder is strongly dependent on the turbulence which exists in the inflow and the turbulence which is created along the wall boundary layer after the stagnation point. In the case where the inflow involves no turbulence, turbulence is created on the wall at a sufficiently high critical Reynolds number, corresponding to the *drag crisis*. This Reynolds number is between $300,000$ and $500,000$. Under this number, the flow is subcritical and, in short the boundary layer flow is laminar. In this case, we put $\theta = 0$ in our model, which means that the VMS-LES model is combined with a laminar boundary layer, an option which is justified when the turbulence arising is essentially wake turbulence. We consider first a rather low Reynolds of 3900 and analyse in which conditions a better prediction is obtained with a very coarse mesh ($290,000$ vertices) and a medium mesh ($1,400,000$ vertices). The WALE SGS is used, and we compare the association of VMS-WALE with dynamic limitation and without. The effect of dynamic limitation results in a global reduction of SGS viscosity, see for example the contours of SGS viscosity obtained at Reynolds $20,000$ which are depicted in Figure 5. Surprisingly, the effect on wake velocity is small in general, but yet rather notable at the limit of wake, see Figures

	Mesh	$\overline{C}_d$	l_r/D	$-\overline{C}_{p_b}$	St
VMS	270K	0.96	1.06	0.94	0.22
VMS dyn.	270K	0.97	1.08	0.93	0.22
VMS	1.4M	0.94	1.47	0.81	0.22
VMS dyn.	1.4M	0.94	1.47	0.85	0.22
LES					
Lee(Min)	7.7M	0.99	1.35	0.89	0.209
Lee(Max)	7.7M	1.04	1.37	0.94	0.212
Kravchenko					
(Min)	0.5	1.04	1.	0.93	0.193
(Max)	2.4M	1.38	1.35	1.23	0.21
Parneaudeau					
(Min)	44M	-	1.56	-	0.207
(Max)	44M	-	1.56	-	0.209
Experiments					
Parneaudeau					
(Min)		-	1.51	-	0.206
(Max)		-	1.51	-	0.210
Norberg					
(Min)		0.94	-	0.83	
(Max)		1.04	-	0.93	
Ong(Min)		-	-	-	0.205
Ong(Max)		-	-	-	0.215

Table 1. Bulk quantities for Re=3900 flow around a cylinder (VMS-WALE vs VMS-WALE dynamic)

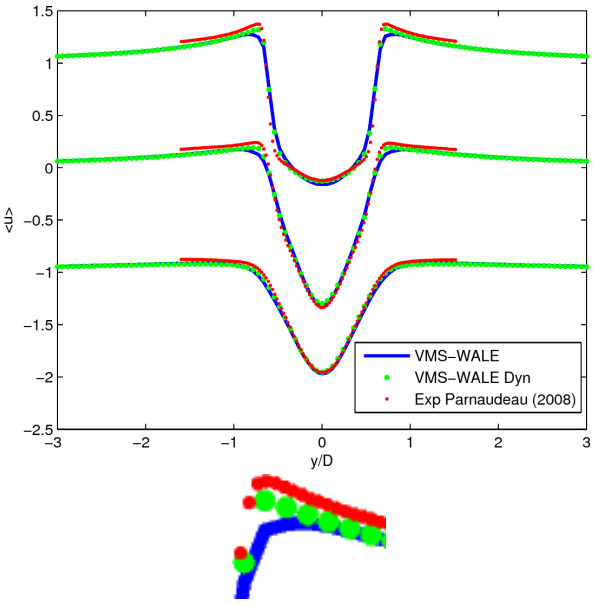

Figure 4. Cylinder, Re=3900: Mean streamwise velocity profiles at $x/D = 1.06, 1.54$ and 2.02 and a zoom of the $x/D = 1.06$ cut (finer grid).

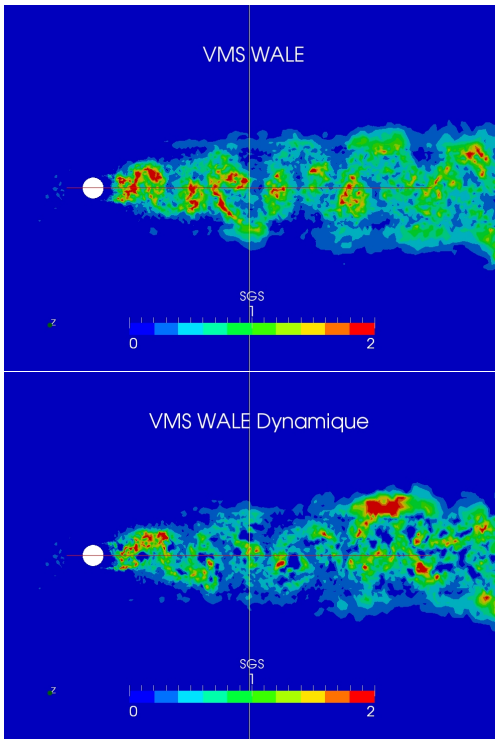

Figure 5. Cylinder, Re=20,000: viscosity ratio μ_{SGS}/μ - non-dynamic VMS versus dynamic VMS

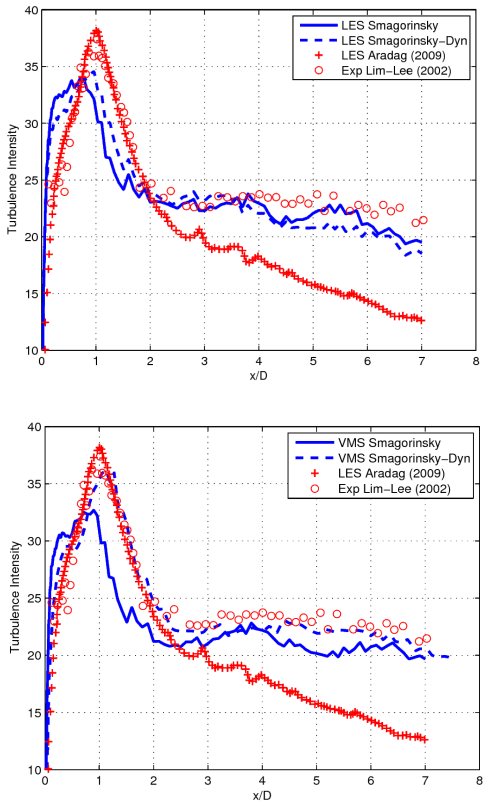

Figure 6. Cylinder, Re=20,000: turbulence intensity in the axis of wake: Dynamic improves LES (top) and strongly improves VMS (bottom).

	Mesh	$\overline{C}_d$	$\frac{l_r}{D}$	St	C'_L	C'_d
VMS:						
	1.2M	2.08	0.74	0.127	1.38	0.25
dyn.	1.2M	2.06	0.82	0.128	1.28	0.24
LES						
(Min)	110K	1.66	0.89	0.07	0.38	0.1
(Max)	3.8M	2.77	2.96	0.15	1.79	0.27
DNS	3.7M	2.1	-	0.133	1.22	0.21
Exp.						
Lyn		2.1	0.88	0.133	-	-
Luo		2.21	-	0.13	1.21	0.18

Table 2. Square cylinder, Re=22,000: Bulk coefficients (LES: Rodi ; DNS: Verstappen)

4. Global coefficients are also slightly improved, see Table 1.

A second example is the flow around the circular cylinder with Reynolds number of 20,000. In Figure 5 we show the rather high variation between the VMS viscosity with and without the dynamic control. The impact of the dynamic procedure on the turbulence intensity along the axis of the wake is important as shown in Figure 6.

6.2. SQUARE CYLINDER

As a second example to show the interest in combining VMS and dynamic control, we computed a classical workshop test case [19]. The incompressible flow around a square cylinder at Reynolds 22,000 and zero angle of attack is considered. The VMS-LES option is applied on a mesh of 1.2M vertices. The influence of the dynamic procedure on the evaluation of the bulk coefficients is quite small, as shown in Table 2 which also compares the current computation with LES results from [20, 21] and measurements from [22, 23, 24]. Conversely the deviation to measurements of the mean velocity profiles is greatly reduced when the dynamic control is used, see Figures 7,8.

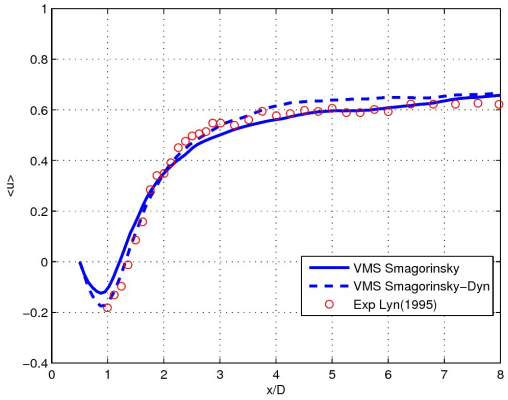

Figure 7. Square cylinder, Re=22K: mean streamwise velocity on the wake center-line.

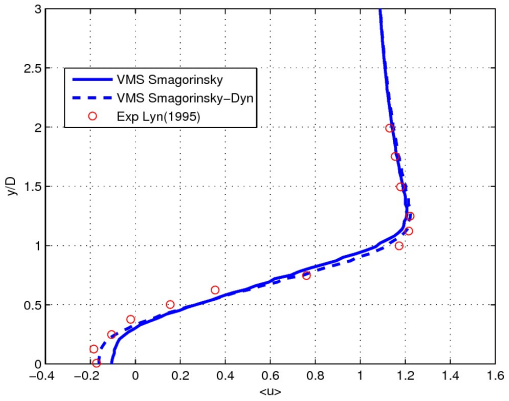

Figure 8. Square cylinder, Re=22K: mean streamwise velocity at $x/D = 1$.

6.3. CIRCULAR CYLINDER - SUPERCRITICAL

We now address the flow around a circular cylinder at a Reynolds 1 million, higher than the critical one. We propose to compare the results of three options, (a) $\theta = 0$, that is RANS, (b) $\theta = 1$, that is VMS-WALE, (c) hybrid RANS-VMS-WALE. Moreover, we try to get reasonable results with a medium-sized mesh of 1.2 million vertices. The available experiments are scarce, [22, 23, 24], and show some scatter. Numerical results are found [20, 21]. They present a even higher scatter (Table 3). Among options (a),(b),(c), we observe that the hybrid calculation is in a rather good agreement with the measurements.

6.4. TANDEM CYLINDERS

The last case concerns the flow around two cylinders in tandem, at Re=1.66×10^5. This test case was studied in an AIAA workshop, see [25]. Among the conclusions of the workshop, adressing this case with LES was considered as a too difficult task with existing computers. Results of DES-based computations were much closer to measurements. We have

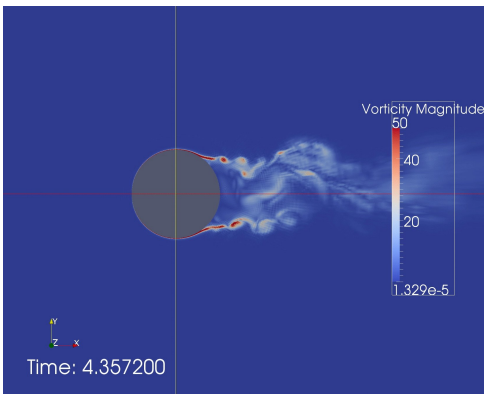

Figure 9. Flow around a circular cylinder at Re=1 million: vorticity field.

	Mesh	$\overline{C}_d$	C'_l	$-\overline{C}_{p_b}$	St
URANS	1.2M	0.24	0.06	0.25	0.46
VMS WALE	1.2M	0.36	0.22	0.22	0.10
Hybrid:					
VMS-WALE	1.2M	0.24	0.17	0.28	0.17
Catalano:					
URANS	2.3M	0.40	-	0.41	0.31
LES	2.3M	0.31	-	0.32	0.35
LES Kim	6.8M	0.27	0.12	0.28	-
Exp.:					
Shih		0.24	-	0.33	-
Gölling		-	-	-	0.10
Zdravkovich:					
(Min)		0.2	0.1	0.2	0.18
(Max)		0.4	0.15	0.34	0.18

Table 3. Flow around a circular cylinder at Rey=1 million: bulk coefficients.

computed the case with a mesh of 2.59M nodes. Two modeling options were considered: (a) RANS and (b) Hybrid VMS-LES-WALE dynamic. An idea of the impact of these options on the resulting flow is proposed in Figure 10. Some comparison of bulk coefficients is given in Table 4 in which the other computational figures are taken from [26] and for Lockard and Aybay from [25]. Experimental outputs are taken from [27]. Drag for the first cylinder shows a small scatter with the various hybrid calculations. The simulation around the second cylinder is more challenging as also illustrated by the pressure distributions (Figure 11).

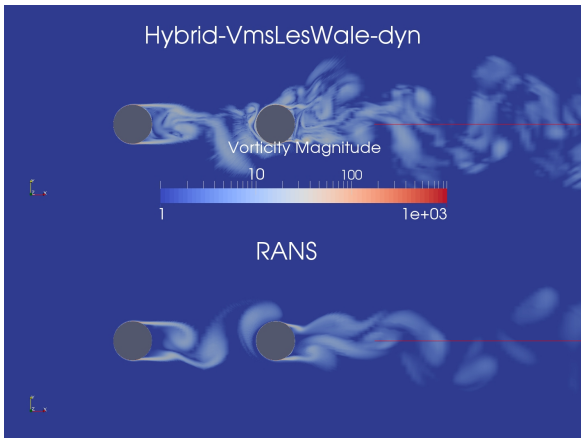

Figure 10. Tandem cylinders: Vorticity magnitude - Hybrid VMS versus RANS.

7. CONCLUSION, PERSPECTIVES

The main effect of dynamic control of SGS viscosity is a significant reduction of the amount of SGS viscosity in VMS-LES. The impact in VMS-LES is smaller than for pure LES but still non-negligible. In a large part of the tested cases we observe that the dynamic procedure brings a sensible improvement to the agreement with reference data. Then a strategy

	Mesh	$\overline{C}_d$ Cyl. 1	$\overline{C}_d$ Cyl. 2
Hybrid VMS dyn.	2.59M	0.64	0.38
Numerical results			
Lockard (2011)	2M-133M	0.33-0.80	0.29-0.52
DES Aybay (2010)	6.7M	0.64	0.44
HRLES Vatsa (2010)	8.7M	0.64	0.45
Experiments		0.64	0.31

Table 4. Tandem cylinders: Bulk coefficients (experimental coefficients are computed by integrating experimental pressure of Neuhart).

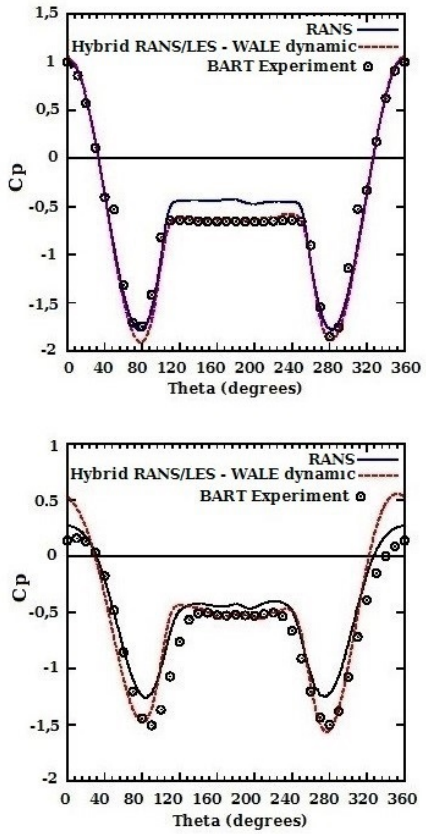

Figure 11. Tandem cylinders: Mean pressure coefficient distribution on the upstream cylinder (top frame) and on the downstream cylinder (bottom frame).

for blending RANS and VMS-LES is presented. The supercritical flow around a circular cylinder is reasonably well predicted by the proposed VMS hybrid model. The tandem cylinder case shows at the same time some improvement and that further research is necessary.

8. ACKNOWLEDGEMENTS

This work has been supported by French National Research Agency (ANR) through project MAIDESC n^o ANR-13-MONU-0010. HPC resources from GENCI-[CINES] (Grant 2010-x2010026386 and 2010-c2009025067) are also

gratefully acknowledged.

REFERENCES

[1] Moussaed, C., Wornom, S., Salvetti, M., Koobus, B., and Dervieux, A., 2014, "Impact of dynamic subgrid-scale modeling in variational multiscale large-eddy simulation of bluff body flows", *Acta Mechanica*, Vol. 1-15.

[2] Moussaed, C., Salvetti, M., Wornom, S., Koobus, B., and Dervieux, A., 2014, "Simulation of the flow past a circular cylinder in the supercritical regime by blending RANS and variational-multiscale LES models", *Journal of Fluids and Structures*, Vol. 47, pp. 114–123.

[3] Spalart, P., Jou, W.-H., Strelets, M., and Allmaras, S., 1997, "Comments on the feasibility of LES for wings, and on a hybrid RANS/LES approach", *Advances in DNS/LES*, pp. 137–147.

[4] Spalart, P., Deck, S., Strelets, M., Shur, M., Travin, A., and Squires, K., 2006, "A new version of detached-eddy simulation, resistant to ambiguous grid densities", *Theor Comput Fluid Dyn*, Vol. 20, pp. 181–195.

[5] Roe, P., 1981, "Approximate Riemann solvers parameters vectors and difference schemes", *J Comp Phys*, Vol. 43, pp. 357–372.

[6] Leer, B. V., 1977, "Towards the ultimate conservative scheme. IV : a new approach to numerical convection", *J Comp Phys*, Vol. 23, pp. 276–299.

[7] Camarri, S., Koobus, B., Salvetti, M., and Dervieux, A., 2004, "A low-diffusion MUSCL scheme for LES on unstructured grids", *Computers and Fluids*, Vol. 33, pp. 1101–1129.

[8] Hughes, T., Mazzei, L., and Jansen, K., 2000, "Large eddy simulation and the variational multiscale method", *Comput Vis Sci*, Vol. 3, pp. 47–59.

[9] Koobus, B., and Farhat, C., 2004, "A variational multiscale method for the large eddy simulation of compressible turbulent flows on unstructured meshes-application to vortex shedding", *Comput Methods Appl Mech Eng*, Vol. 193, pp. 1367–1383.

[10] Nicoud, F., and Ducros, F., 1999, "Subgrid-scale stress modelling based on the square of the velocity gradient tensor", *Flow, Turbulence and Combustion*, Vol. 62, pp. 183–200.

[11] Germano, M., Piomelli, U., Moin, P., and Cabot, W., 1991, "A dynamic subgrid-scale eddy viscosity model", *Phys Fluids A*, Vol. 3 (7), pp. 1760–1765.

[12] Lilly, D., 1992, "A proposed modification of the Germano subgrid-scale closure method", *Phys Fluids*, Vol. A4, p. 633.

[13] Goldberg, U., and Ota, D., 1990, "A $k-\varepsilon$ Near-Wall Formulation for Separated Flows", *Tech. Rep. 91–1482*, AIAA 22nd Fluid Dynamics, Plasma Dynamics & Lasers Conference.

[14] Lee, J., Park, N., Lee, S., and Choi, H., 2006, "A dynamical subgrid-scale eddy viscosity model with a global model coefficient", *Phys Fluids*, Vol. 18 (12).

[15] Kravchenko, A., and Moin, P., 1999, "Numerical studies of flow over a circular cylinder at Re=3900", *Phys Fluids*, Vol. 12 (2), pp. 403–417.

[16] Parneaudeau, P., Carlier, J., Heitz, D., and Lamballais, E., 2008, "Experimental and numerical studies of the flow over a circular cylinder at Reynolds number 3900", *Phys Fluids*, Vol. 20 (085101).

[17] Norberg, C., 1987, "Effects of Reynolds number and low-intensity free-sream turbulence on the flow around a circular cylinder", *Publ No 87/2, Department of Applied Termosc and Fluid Mech, Chalmer University of Technology, Gothenburg, Sweden*.

[18] Ong, L., and Wallace, J., 1996, "The velocity field of the turbulent very near wake of a circular cylinder", *Exp Fluids*, Vol. 20, pp. 441–453.

[19] Rodi, W., Ferziger, J. H., Breuer, M., and Pourquié, M., 1997, "Status of large eddy simulation: results of a Workshop", *ASME J Fluids Eng*, Vol. 119, pp. 248–262.

[20] Wang, M., Catalano, P., and Iaccarino, G., 2001, "Prediction of high Reynolds number the flow over a circular cylinder using LES", *Annual research briefs*, Center for Turbulence Research, Stanford.

[21] Kim, S.-E., and Mohan, L., 2005, "Prediction of unsteady loading on a circular cylinder in high Reynolds number flows using large eddy simulation", *Proceedings of OMAE 2005: 24th International Conference on Offshore Mechanics and Artic Engineering, june 12-16, Halkidiki, Greece, OMAE 2005-67044*.

[22] Shih, W., Wang, C., Coles, D., and Roshko, A., 1993, "Experiments on flow past rough circular cylinders at large Reynolds numbers", *J Wind Eng Indust Aerodyn*, Vol. 49, pp. 351–368.

[23] Goelling, B., 2006, "Experimental investigations of separating boundary-layer flow from circular cylinder at Reynolds numbers from 10^5 up to 10^7; Three-dimensional vortex

flow of a circular cylinder", G. Meier, and K. Sreenivasan (eds.), *Proceedings of IUTAM Symposium on One Hundred Years of Blound-ary Layer Research*, Springer, The Netherlands, pp. 455–462.

[24] Zdravkovich, M., 1997, *Flow around circular cylinders Vol 1: Fundamentals.*, Oxford University Press.

[25] Lockard, D., 2011, "Summary of the Tandem Cylinder Solutions from the Benchmark Problems for Airframe Noise Computations-I", *Proceedings of Workshop AIAA-2011-353*.

[26] Vatsa, V., and Lockard, D., 2010, "Assessment of Hybrid RANS/LES turbulence models for areoacoustics applications", *AIAA Paper*, Vol. 2010-4001.

[27] Neuhart, D., Jenkins, L., Choudhari, M., and Khorrami, M., 2009, "Measurements of the flowfield interaction between tandem cylinders", *AIAA Paper*, Vol. 2009-3275.